

# Roll to roll fabrication technologies for optoelectronic and electronic devices and sensors

A. Maaninen\*, M. Tuomikoski, L. Kivimäki, T. Kololuoma, M. Välimäki, M. Leinonen, M. Käsäkoski

VTT Electronics, Kaitoväylä 1, FIN-90571 Oulu, Finland

## ABSTRACT

Embedding of optoelectrical, optical, and electrical functionalities into low-cost products like product packages and printed matter can be used to increase their information content. For these purposes, components like displays, photodetectors, light sources, solar cells, battery elements, diffractive optical elements, light guides, electrical conductors, resistors, transistors, switching elements etc. and their integration to functional modules are required. Also the need of rapid and reliable diagnostic systems for wellness and healthcare applications is apparent. Today the time from sampling to result can take hours or even several days. In future the target is to analyze the sample within a few minutes for further action. Additionally, the price of the components for low-end products and disposable sensors has to be in cent scale or preferably below that. Therefore, new, cost-effective, and volume scale capable manufacturing techniques are required. Recent developments of liquid-phase processable electrical and optical polymeric, inorganic, and hybrid material inks together with biocompatible materials have made it possible to fabricate functional components by conventional roll-to-roll techniques such as gravure printing on flexible paper and plastic like substrates. In this paper, we show our current achievements in the field of roll-to-roll fabricated electronics, optoelectronics and biosensors. With examples of light guiding structures, organic light emitting diodes, biocompatible materials, we demonstrate the huge potential of roll to roll fabrication as a low cost mass production technology for future low end electronic products.

**Keywords:** Roll-to-roll, gravure printing, light-emitting diode, biosensor, light guide

## 1. INTRODUCTION

Gravure printing has introduced one of the fast and cost effective roll-to-roll techniques with adequate patterning resolution and low process temperature. In this technique the pattern to be printed is engraved into the rotational printing cylinder. The engraved cells are filled with ink that is transferred to the foil when the cylinder is brought into contact with the surface of foil. During printing the excess ink is removed from the cylinder by the use of the flexible doctor blade. This ensures that the cells are filled with exact volume of ink.



Figure 1. Photographs of (a) a table-top size gravure printer, and (b) a doctor blade and cylinder with engraved cells.

\* Arto.Maaninen@vtt.fi; phone +358 (0)20 722 2348; fax +358 (0)20 722 2320; www.vtt.fi

In this study, a table top gravure printer (Figure 1(a)) was used for printing experiments. The printer has a cylinder with engraved cells and flexible doctor blade tools, which are shown in Figure 1(b). The printing force and speed can be varied from 100 N to 1000 N and from 6 to 60 m/min, respectively.

## 2. POLYMER LIGHT-EMITTING DEVICES

$\pi$ -conjugated polymers are very promising and attractive materials for use in electroluminescent displays<sup>1</sup>, photovoltaics, transistors, and sensors, because they combine the optoelectronic properties of semiconductors with the processing advantages and mechanical properties of plastics. Currently, processing and fabrication of thin films for polymer electronics is carried out using traditional techniques such as spin coating. However, these techniques have several disadvantages, e.g. material wastage and time consuming, and therefore, tremendous benefits are gained by incorporating printing technique in the deposition of polymer thin films.<sup>2,3</sup>

In this study, our interest is to print light-emitting thin films for the flexible polymer light-emitting device using semiautomatic table-top size gravure printer. It is known that the electroluminescence performance of the device is highly sensitive to the film morphology. For the examination of printed films, an experimental design was used as a help of minimising the number of experiments.

### 2.1. Experimental design

The experimental design makes it possible to describe the system's behaviour on the examined region with the help of a mathematical model. The model construction is based on factors and responses. The purpose of the experimental design is to evaluate which experiments are important in order to minimize the number of necessary experiments. The experimental design was carried out with Modde 6.0 program.

The factors are usually chosen based on existing information. Therefore, in order to attain a reliable model it is important to understand the system generally. The variables are required to be independent, so they should not interact with each other. In order to describe the behaviour of the gravure printing process, the determination of the most significant factors and their levels, as well as the most descriptive responses, was needed. On the grounds of the preliminary information, the concentration of the polymer, the solvent ratio, the speed of the roll, the pressure force against the roll and the cell size on the surface of the roll were considered to impact most on the examined process. All relevant responses should be included in the design. The responses can hold either measured data or information based on evaluated opinion. The number of variables will influence the number of experiments. An increase in the number of variables will expand the experimental design, but the responses will have no influence on the number of experiments.

According to the model, the MEH-PPV concentration and cell depth influences most on the layer thickness as shown in the response surface in Figure 2. The increased MEH-PPV concentration and larger cell size increases the layer thickness. Solvent ratio, the pressure force and the roll speed were not observed to have a significant effect on the model. The reliability of the model was tested in practice against the response surface by printing polymer using different cell depths and concentrations. The results showed that the giving model can predict the film thickness accurately.

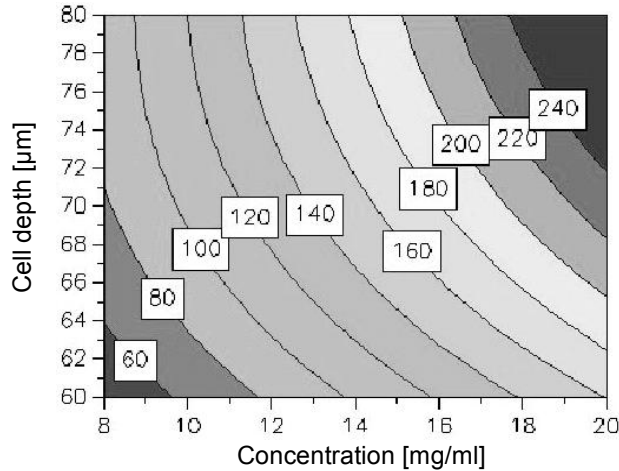


Figure 2. Cylinder cell depth versus polymer concentration response surface of gravure printed MEH-PPV film. The thickness of films varied from 60 nm to 240 nm.

After examination of thickness of printed polymer films, the surface profiles were determined. Figure 3(a) shows one centimeter cross sections of four printed surfaces with different film thickness. 62 nm, 91 nm, 118 nm, and 189 nm thick films were achieved with a roughness mean square, RMS, of less than 4 nm in all films. The surface profiles are being measured along films, and they are not showing any significant holes or bumps in the surface. Furthermore, white light interferometer was used to illustrate the surface of polymer film, as shown in Figure 3(b).

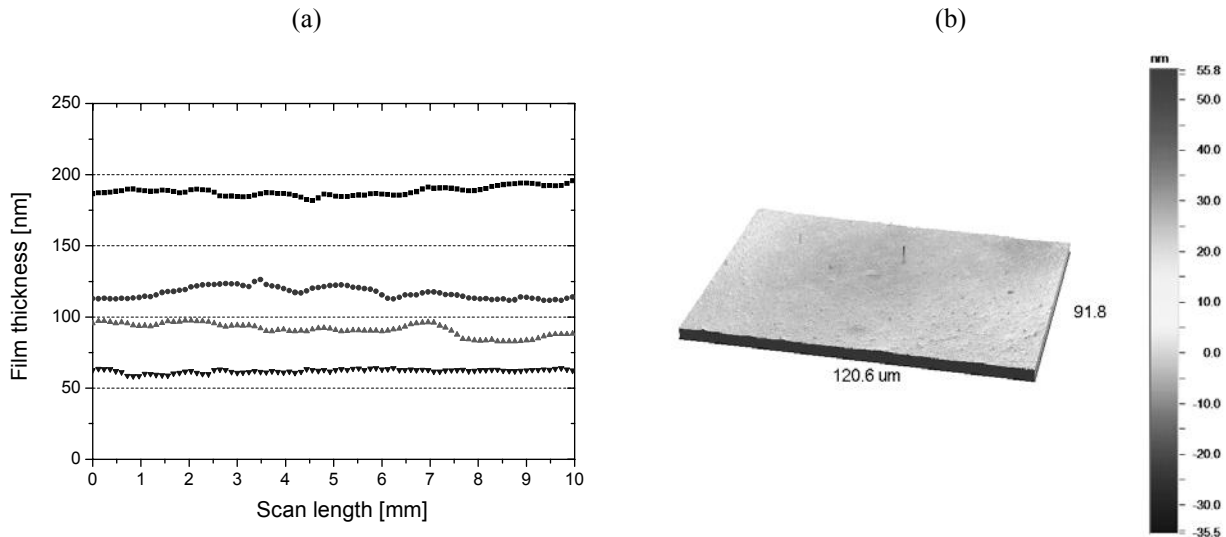


Figure 3. (a) Surface profile from cross section of printed MEH-PPV films. Thickness of films were 62nm, 91nm, 118 nm, and 189 nm with low RMS of <4 nm. (b) 3D surface profile of polymer film from the area of 0.011 mm<sup>2</sup>.

## 2.2. Fabrication of polymer LED

The PLED structure studied consisted of ITO/PEDOT/MEH-PPV/Ca/Al as shown in Figure 4. For the hole injection layer the conductive polymer, poly(3,4-ethylenedioxythiophene) doped in poly(styrenesulfonate) (PEDOT:PSS) was spin coated resulting 70-nm thick film onto precleaned poly(ethyleneterephthalate) (PET) substrate coated with indium-tin-oxide (ITO, 50 ohms-sq<sup>-1</sup>) anode. The film was subsequently dried at 60°C for over night in N<sub>2</sub> atmosphere. Poly[2-

methoxy-5-(2-ethylhexyloxy)-1,4-phenylenevinylene] (MEH-PPV, Mw ~280'000 g/mol) was utilized as an active luminescent material.

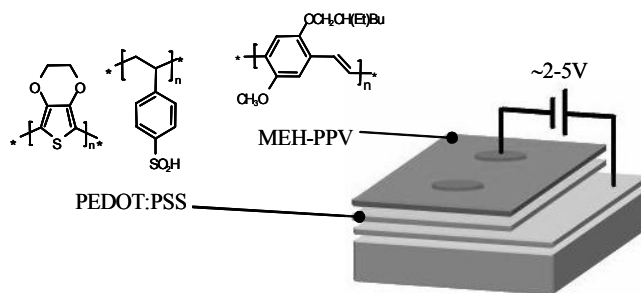


Figure 4. Molecular structures of PEDOT:PSS and MEH-PPV polymers and device structure of polymer LED. Usually applying 2-5 volts between electrodes generates light emission from the emitting polymer.

The polymer solution was gravure printed at the speed of 60 m/min and followed by drying at 60°C for 2 hours in N<sub>2</sub> atmosphere. The Ca/Al cathode was prepared by vacuum evaporation at the base pressure of 10<sup>-6</sup> mbar. The circle emitting area was 16 mm<sup>2</sup>.

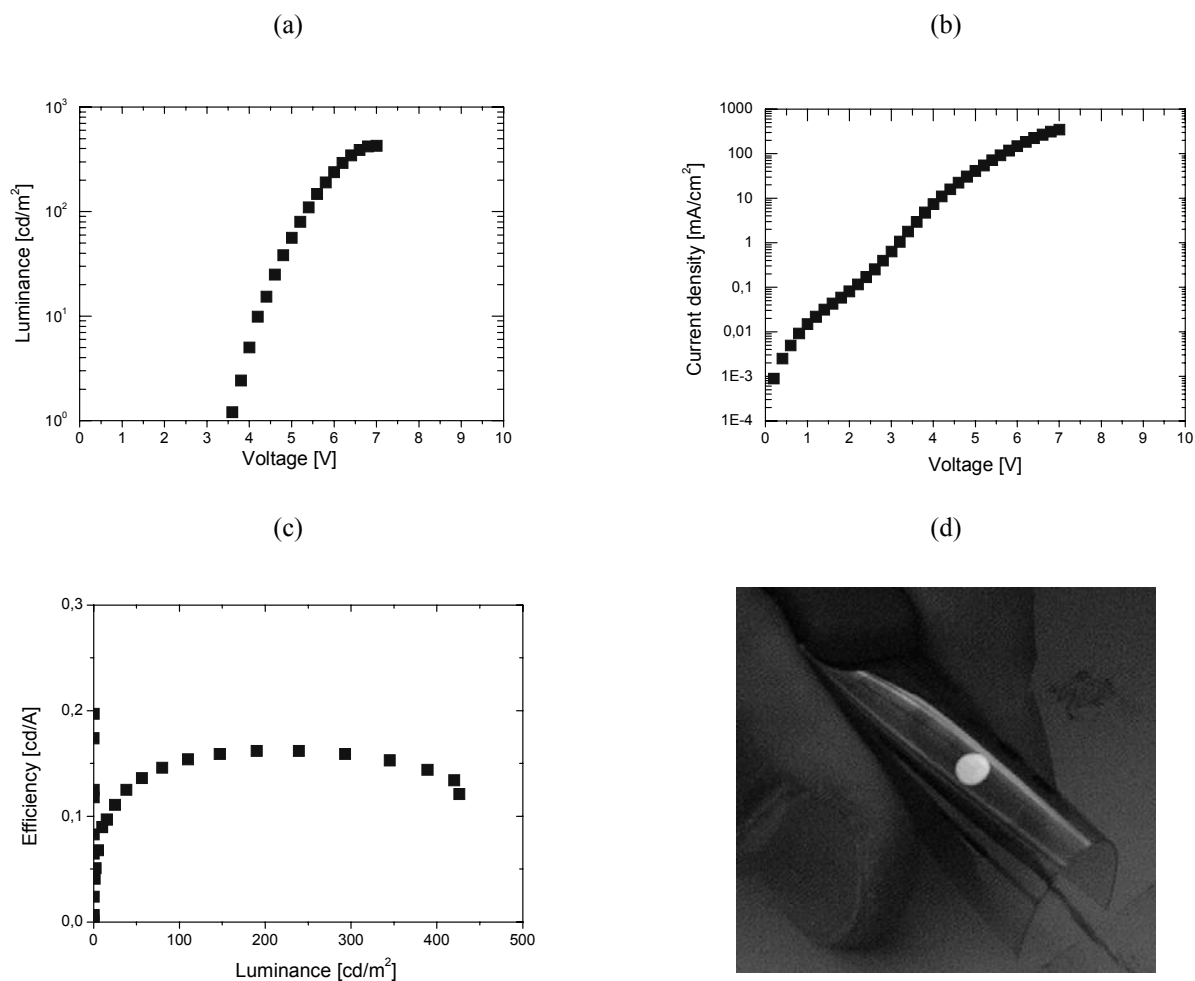


Figure 5. (a)-(c) *I-L-V* and efficiency characteristics of printed polymer LED. (d) Photograph of emitting PLED pixel.

One of gravure printed light-emitting film with thickness of 91 nm was used to fabricate the PLED. The current density-luminance-voltage ( $I-L-V$ ) and efficiency measurements were carried out in room ambient condition with epoxy encapsulation, and their characteristics are shown in Figure 5. The turn-on voltage for light emission at  $1 \text{ cd/m}^2$ , and brightness of  $100 \text{ cd/m}^2$  were observed at 3.6V and 5.4V, respectively. Very low current densities at low voltages, 0-2V, indicates pin-hole free films with good uniformity. Maximum current efficiency of 0.16 cd/A was achieved.

### 3. BIOSYSTEMS

New simple and reliable tools are required for the health care system to reduce the number of costly laboratory tests and hospital controls. Also self care, such as individuals own responsibility and attention of their health and fitness, requirements are increasing. One approach is to provide cost-effective and sensitive lab-on-a-chip biosensors.

The aim of this study was to generate biomolecule containing matrixes which retain their activity after gravure printing process. Biocompatible matrixes were developed via the sol-gel technique.<sup>4</sup> The advantages of sol-gel technique include e.g. simplicity and mildness of the process. Additionally, doping of the biomolecules in the sol-gel reduces processing steps when both components can be processed to one coating instead of two separate layers.

#### 3.1. Sol-gel synthesis and biomolecule doping

Tetraethyl orthosilicate (TEOS), (3-glycidoxypropyl)trimethoxysilane (GPTS), hydrochloric acid (HCl) and 5 m% AlO(OH) in water were reacted with stirring to form the sol-gel matrix (see Figure 6). Nanoparticle AlO(OH) (boehmite) was used to catalyze the epoxy ring opening and to accelerate reaction between TEOS and GPTS. Propyltrimethoxysilane (PTMS) was used additionally in some reactions to enhance flexibility of the produced coating. Subsequently the alcohol and water formed during the synthesis were evaporated. The resulting material was dissolved to ethyl alcohol or to another organic solvent. pH of the sol-gel was raised with a buffer near the physiological value in order to retain the activity of the biomolecule.

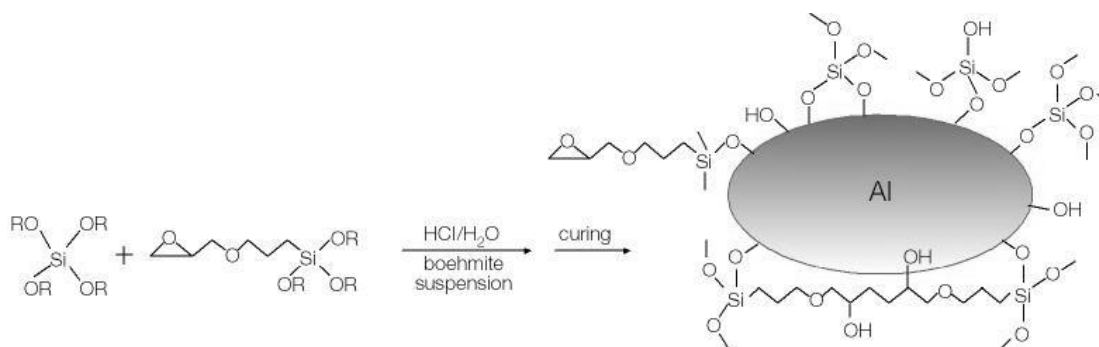


Figure 6. Si-O-Si network formation on the surface of nanoparticle AlO(OH).

Other precursors were also tested but the most sensitive combination was achieved with the above mentioned chemicals. Molar ratio of the precursors, reaction time and temperature affected the sol-gel characteristics, as shown also in several publications.<sup>5,6,7</sup>

Biomolecule containing matrix was achieved by doping the biomolecules in the sol-gel simply by mixing the sol-gel and biomolecules together and curing the formed layer. In another way the sol-gel forms the first layer and the biomolecules are immobilized on top of the cured sol-gel coating (passive coating). In the case of passive coating, the excess antibody was washed away with phosphate buffer. Schematic of experimental arrangement is shown in Figure 7. The antibodies used were mouse IgG and anti-testosterone Fab.

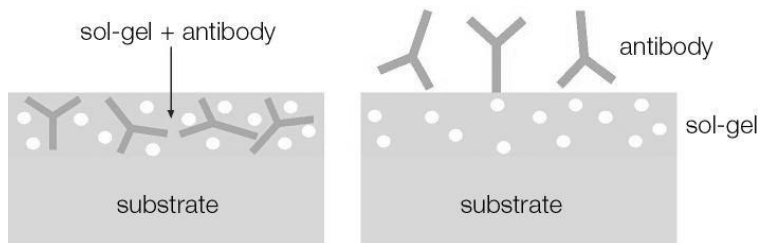


Figure 7. Principle of antibody doping (left) and passive coating (right).

Bioactivity was checked with fluorescence immunoassay. Microtiter well plates were oxygen plasma etched to enhance the adhesion of the sol-gel matrix to the plastic plate. Certain dilutions of the biomolecule were doped with the sol-gel matrix and distributed in the wells. The filled plates were cured at 37°C for four hours in the case of antibody doped materials. When the plate wells had only sol-gel layers for passive coating the layers were cured at 70°C over night.

The amount and activity of the antibodies combined with the sol-gel were detected with fluorescein (FITC; excitation 485 nm, emission 535 nm) labeled anti-IgG antibody or testosterone. When different dilutions of the antibody were used in doping or passive coating, same amount of anti-mouse-IgG-FITC was added to every microwell to identify the antibody. When every microwell had the same amount of anti-testosterone Fab doped in the sol-gel then the detection was done with different testosterone-FITC dilutions. Testosterone-FITC binds specifically to anti-testosterone Fab and shows the activity of the biomolecule. Nonspecific binding of the label complex was inhibited with BSA protein (bovine serum albumin) before the label insertion. The label complex was attached and excess washed away with buffer. Fluorescence was measured by Victor 2V platereader (Wallac).

### 3.2. Material development and biomolecule doping

Examples of the fluorescence of passive coated and doped antibodies are seen in Figure 8(a) and (b), respectively. In Figure 8(a) different amounts of IgG were passively immobilized on the cured sol-gel coating. The fluorescence response is even four to five times higher compared to the regular microtiter well. As shown in Figure 8(b) the fluorescence response followed the testosterone-FITC dilutions. Anti-testosterone Fab retained its activity in the sol-gel.

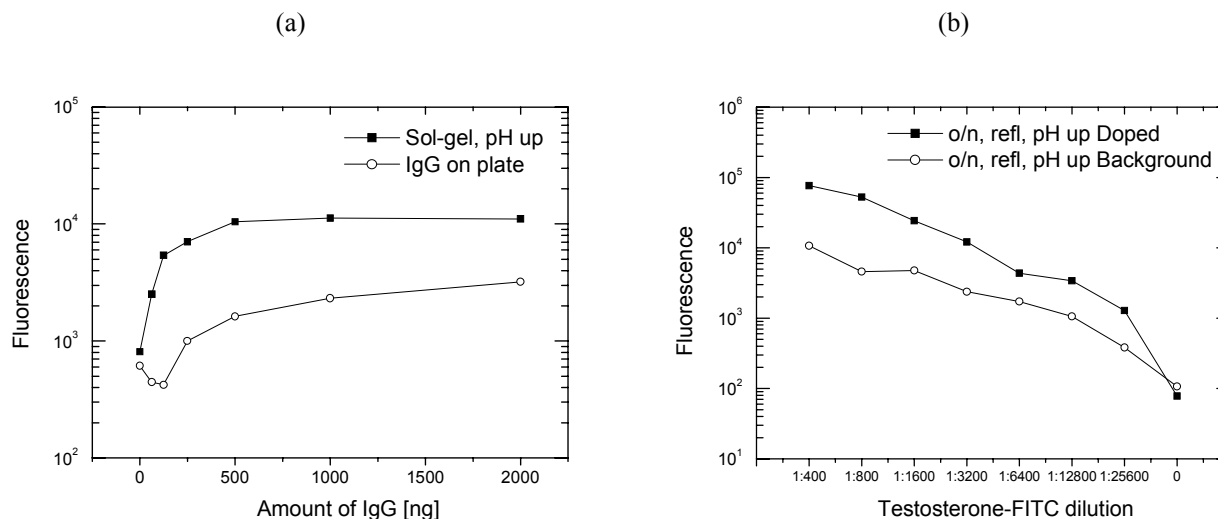


Figure 8. Plots of (a) mouse IgG passively coated on the cured sol-gel, detection with anti-mouse-IgG-FITC, and (b) sol-gel doped with anti-testosterone-Fab, detection with testosterone-FITC.

### 3.3. Printing test

The obtained biomolecule (mouse IgG) containing sol-gel material was printed on polystyrene slides which were plasma etched before use to achieve better adhesion of the material on the plastic sheet. A table top gravure printing machine (Figure 1(a)) was used for printing tests

The appearance of immobilised IgG in sol-gel was checked with fluorescence measurement using Alexa Fluor 546 labelled antibodies specific to the printed IgG-sol-gel –coating. To prevent nonspecific binding, the slides were treated with BSA protein (bovine serum albumin). Fluorescence was detected with Molecular Imager FX Pro equipment (Bio-Rad) using excitation/emission wavelengths 532/555 nm, respectively. In quantitative IgG measurements, equal volumes of sol-gel and IgG dilution were mixed. The amounts of IgG on the slides were calculated from the used volumes, which inevitably gives too large detected IgG values for the whole slides.

Sol-gel material with a doped antibody can be printed successfully with a table-top gravure printing machine. With optimisation of machine parameters, smooth sol-gel layers were obtained. The immobilisation of antibody IgG to sol-gel has been investigated during the biocompatible material development, and the immobilisation was found to be effective. With these printing tests we have shown that IgG stays immobilised in the sol-gel also after the gravure printing process. Non-specific binding of the label to the sol-gel was tested with plain sol-gel surfaces (no IgG) using BSA for the blocking agent. According to these tests, the fluorescently labelled antibody does not bind non-specifically to the sol-gel. Thus BSA blocking could be left out, which will reduce the treatment steps. Quantitative sol-gel doped antibody measurement is possible as can be seen in Figure 9(a)-(c). Different concentrations of immobilised IgG in sol-gel could be detected, but the exact limit is not yet defined. Dark and quite large spots come from the glass substrate.

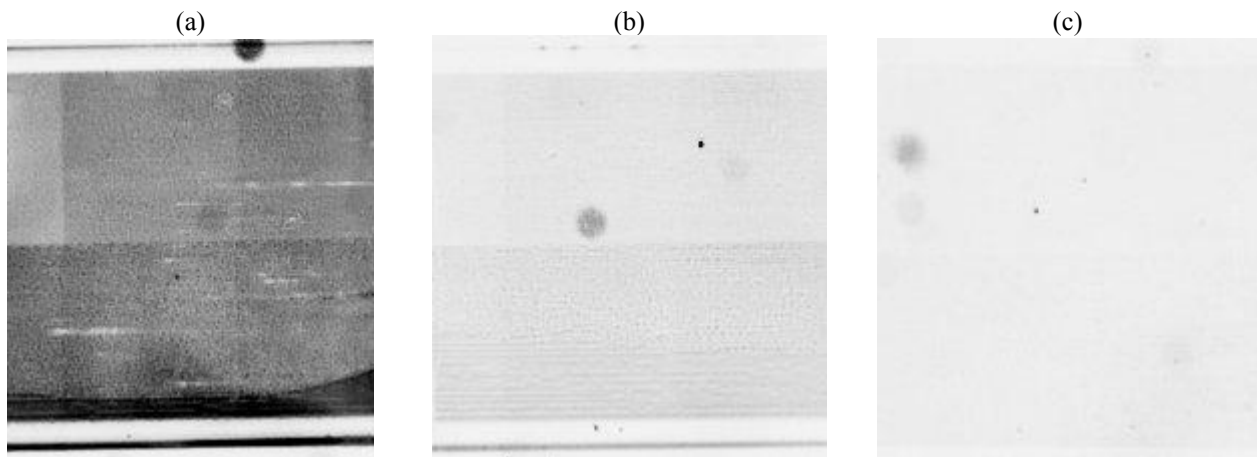


Figure 9. Different amounts of IgG immobilised to the sol-gel mixture: (a) 12 micrograms and (b) 1.5 micrograms, and (c) 0.2 micrograms (not detected). The exact detection limit of IgG in the layer has not been determined.

## 4. FABRICATION OF OPTICAL PLANAR WAVE GUIDES

The aim of the gravure-printed optical light guides was the fabrication of light guiding structures to be used in decorative purposes in product packages. For that purpose the optical attenuation in the light guide does not need to be below 0.1 dB/cm as in the case of light guides for optical telecommunications. Instead, optical attenuation values around 1-2 dB/cm are acceptable.

For the ink fabrication (optical core) commercial polymer materials were used. The aim was to fabricate inks having as high polymer content as possible in order to print light guides with the maximal height and aspect ratio. The first material used was polyvinylpyrrolidone (PVP) grade K15 having low molecular weight ( $M_w \sim 10\,000$ ). PVP was chosen due to its refractive index value ( $n = 1.53$ ), low molecular weight allowing high solid content in ink and good solubility in polar solvents such as water, isopropanol etc. The second core forming polymer was cyclo-olefinic co-polymer (COC,  $n =$

1.53, optical loss in 90  $\mu\text{m}$  film 0.6 dB/cm) known as Topas from Ticona. COC was selected due to its good optical properties (low optical attenuation). From the tested COC grades, grade 8007 showed the best solubility in aromatic solvents and therefore inks were made only from that type of COC. Cellulose acetate film ( $n = 1.46$ ) with the thickness of 95  $\mu\text{m}$  was used as a substrate during the printing experiments.

Printing cylinders for the gravure-printing of the light guides were custom made. Continuous lined cylinders were fabricated by machine tooling at VTT Electronics and by photolithography process at the University of Oulu. Both type of cylinders contained lines with variable widths. According to printing tests it was early noticed that the photolithographically patterned cylinders resulted better quality lines than machine tooled cylinders. Therefore, photolithographically patterned cylinder was used during the test. In Table 1, designed and measured line widths together with line depths are shown.

Table 1. Designed and measured line widths and measured line depths in photolithographically patterned printing cylinder

Designed line width (mm)	Measured line width (mm)	Measured line depth ( $\mu\text{m}$ )
0.1	0.15	30
0.25	0.3	50
0.5	0.55	60
0.75	0.82	65

Light guides having theoretical width of 300  $\mu\text{m}$  were characterized. The white light interferometer Veeco NT3300 was used for the determination of the profile and surface roughness of the light guides. For the determination of the optical losses red light (He-Ne laser) was butt-coupled from the single mode fiber into the light guide and collected with 200 $\mu\text{m}$  core diameter fiber, which was connected to optical power meter and the transmittance was calculated. Transmittance of the light guide was determined using cut-back method.

#### 4.1. PVP

The best quality light guides were fabricated using ink containing 1 g of PVP in ethyl acetate – 2-isopropoxyethanol mixture (total volume of the solvents were 2 ml with 1:1 proportion). The profile of the light guide is shown in Figure X. The height of the channel was about 6  $\mu\text{m}$  and the width 370  $\mu\text{m}$ , being 23 % wider than the groove in the printing roll. The surface roughness determined from the top of the light guide was 15 nm.

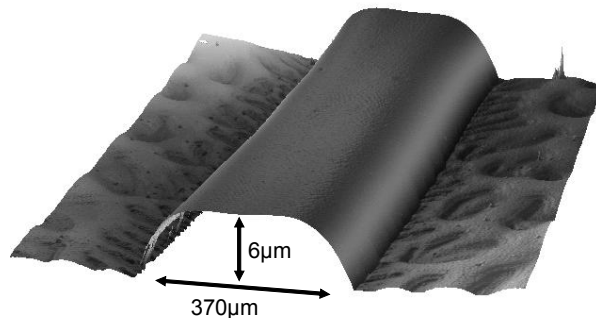


Figure 10. The profile of the gravure printed PVP-based light guide.

According to morphological characterization the surface roughness of the light guide seem to be at the acceptable level. The profile of the light guide is not ideal (smooth edges) and the residuals around the light guide, resulting from the insufficient doctoring during the printing, can be also clearly detected which cause some power spreading in horizontal direction and therefore increase the optical losses. The results obtained from the optical attenuation measurements indicate the optical attenuation of 2.2 dB/cm with rather high, 9.7dB, coupling loss.

## 4.2. COC

The first light guide structures using COC-based ink contained 1 g of COC 8007 in 5.5 ml of o-xylene. According to the morphological analysis channel heights were 2-3 $\mu\text{m}$  but they also contained  $\sim 5\mu\text{m}$  bulges at the edges of the channel as shown in Figure 11(a) and (b). Due to those bulges, clear beam propagation was not observed during the optical characterization.

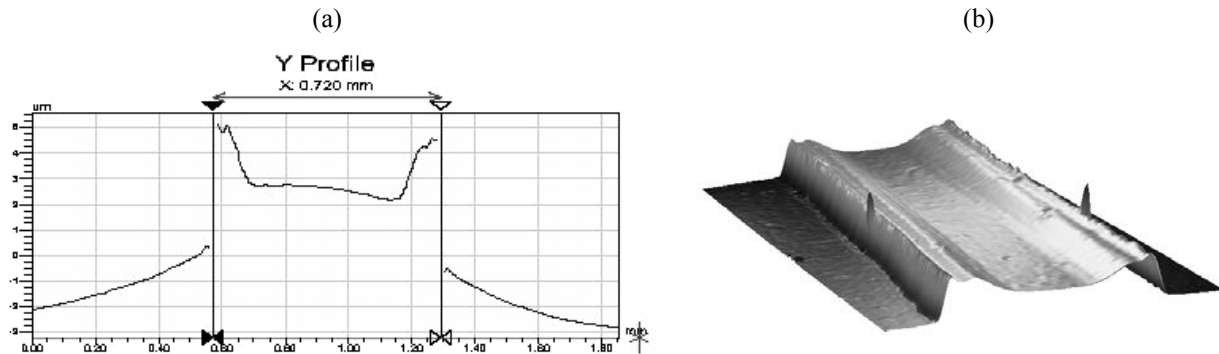


Figure 11. (a) 2D and (b) 3D profiles of the gravure printed COC-based light guide.

The origin of the bulges was thought to be too rapid evaporation of solvent. Therefore, new inks were fabricated using solvents with lower evaporation rates giving more time for the ink to “settle” reducing the height of the bulges. According to obtained results above mentioned procedure enhanced the quality of the channels. The heights of the bulges were reduced to the couple of micrometers but they are still clearly seen.

Optical loss of the light guides fabricated using COC polymers was also measured using the cut back method. According to obtained results the optical loss due to the absorption and scattering was rather low, being only 1.8 dB/cm.

## 5. CONCLUSIONS

In conclusion, the experimental design concept can be used as an effective and helpful tool for the examination and optimization of thin film properties in R2R manufacturing processes. In summary, polymer LEDs based on gravure printed light-emitting polymer films were fabricated successfully. The printed thin films achieved flat uniformity over large area showing the capability to use roll-to-roll manufacturing for thin film based flexible polymer LEDs.

Our results prove that the developed sol-gel materials are biocompatible and can be printed also when an antibody is immobilised to the sol-gel. To our knowledge, this is the first time sol-gel doped antibodies have been successfully gravure printed. According to our tests, it is possible to differentiate IgG amounts from slides but the exact limit for a detectable antibody is still unknown. Our results suggest that the fluorescence label does not bind non-specifically to the sol-gel, which simplifies sample treatment for fluorescence detection.

The gravure printing of light guide channels using direct line printing cylinders has found to be successful. The optical losses for the PVP based light guide channels was 2.2 dB/cm and for COC based channels 1.8 dB/cm. Keeping mind the profile of the COC light guide channels it is strongly believed that light guides with optical losses around or even below 1 dB/cm can be achieved. However, more work is required in order to achieve that kind of level.

## ACKNOWLEDGMENTS

TEKES - National Technology Agency of Finland (PRINTO project), the European Commission (IST004315, ROLLED project) and the European Regional Development Fund, the Provincial State Office of Oulu and the city of Oulu are highly acknowledged for funding the work presented on this paper.

## REFERENCES

1. H. Burroughs, D. D. C. Bradley, A. R. Brown, R. N. Marks, K. Mackay, R. H. Friend, P. L. Burns, and A. B. Holmes, *Nature* (London), **347**, 539, 1990.
2. T. Kololuoma, M. Tuomikoski, T. Mäkelä, J. Heilmann, T. Haring, J. Kallioinen, J. Hagberg, I. Kettunen, and H. Kopola, *Proceedings of SPIE, 5363 Emerging Optoelectronic Applications*, pp. 77-85, 2004.
3. M. Tuomikoski, G. E. Jabbour, T. Kololuoma, and H. Kopola, *Proceedings of Optics Days 2004*, 67, 2004.
4. C. J. Brinker, and G. W. Scherer, *Sol-Gel Science*, Academic Press, San Diego, 1990.
5. M. T. Reetz, *Adv. Mater.*, **9**, no 12, pp. 943-954, 1997.
6. T. Keeling-Tucker and J. D. Brennan, *Chem. Mater.*, **13**, pp. 3331-3350, 2001.
7. N. Rupcich, A. Goldstein, and J. D. Brennan, *Chem. Mater.*, **15**, pp. 1803-1811, 2003.